Optimization of the structural and process parameters in the sheet metal forming process[†]

Jae-Jun Lee[1] and Gyung-Jin Park[2,*]

[1]*Department of Mechanical Engineering, Hanyang University, 17 Haengdang-dong, Seongdong-gu, Seoul, 133-791, Korea*
[2]*Department of Mechanical Engineering, Hanyang University, 55 Hanyangdaehak-ro, Sangnok-gu, Ansan City, Gyeonggi-do, 426-791, Korea*

Abstract

The quality of the sheet metal forming product is determined by defects such as wrinkling, springback, etc. Optimization techniques can avoid such defects while the desired final shape is obtained. The design variables of the optimization process consist of the structural parameters and process parameters. The structural parameters are the initial blank shape, geometry, etc. and the process parameters are the blank holding force (BHF), the drawbead restraining force (DBRF), etc. In this paper, the two groups of parameters are separately optimized. The structural parameters are optimized by the equivalent static loads method for non linear static response structural optimization (ESLSO) and the process parameters are optimized by the response surface method (RSM). A couple of examples are solved by the iterative use of ESLSO and RSM, and the solutions are discussed.

Keywords: Equivalent static loads (ESL); Equivalent static loads method for non linear static response structural optimization (ESLSO); Sheet metal forming; ESLs for the nonlinear strains; Response surface method (RSM)

---

1. Introduction

The product of the desired shape is made by the plastic deformation of the material in the sheet metal forming process. However, the defects of a workpiece occur due to wrinkling, springback, material failure and others [1]. The problems of the defects can be improved by optimization of the metal forming process. Two kinds of design variable groups exist in this optimization; one is the structural parameter group and the other is the process parameter group. The structural parameters are the initial size, shape of the blank, etc. which are the geometries of the workpiece. The process parameters are the working conditions such as the punch velocity, the blank holding force (BHF), the drawbead restraining force (DBRF), the drawbead length (DBL), the friction factor, etc.

A different optimization method is employed for each group of the parameters. Researches on the optimization of structural parameters are typically based on an interpolation method [2-5], an inverse finite element method [6-8] and others [9-12]. The research goal using these methods is to determine the initial blank shape for the desired final shape. When the plastic deformation path of metal and other parameters are not considered exactly, these researches have the disadvantages of

increasing errors and overlooking material failure. Researches on the optimization of the process parameters are typically based on a probabilistic (design of experiments (DOE)) or an approximation method (response surface method (RSM)) [13, 14]. These methods are not mathematically complicated and are easier than the conventional method using gradient information. Optimization of the process parameters is employed when the wrinkling and springback phenomena should be improved and material failure is considered [13-16].

Researches on optimization considering both groups of parameters are not studied much. DOE or RSM can be used when the structural and process parameters are simultaneously considered. Many design variables, which can control the blank shape, are typically involved in determining the detailed shape. Therefore, these methods are quite expensive because many nonlinear analyses are required when the number of design variables is large.

In this research, the sheet metal forming process is optimized considering both the structural and the process parameters. Two groups of parameters are separately optimized by structural optimization and RSM, respectively. The two optimization processes iteratively proceeds until the convergence criteria are satisfied. The initial blank shape, which is the structural parameter, is determined as the desired final shape after the forming process by using structural optimization under the given process parameters. The process parameters

---

such as BHF, DBRF and DBL are optimized by using RSM. Because BHF, DBRF and DBL are the input in conventional structural optimization, they cannot be used as design variables. On the other hand, they can be used as the design variables in RSM. Moreover, since the number of process variables is small, RSM can be exploited to determine the process variables. Finite element analysis is utilized to evaluate the sheet metal forming process in optimization [1-16].

An optimization problem is formulated and solved with the structural and the process parameters as the design variables. In optimization using structural optimization, the structural parameters are only used as the design variables. In optimization using RSM, only the process parameters are used as the design variables. Wrinkling, springback and material failure are considered in the optimization formulation. A new approach is required when the structural parameters are optimized. This is because the formulated optimization is nonlinear dynamic response optimization and considers some phenomena. The equivalent static loads method for non linear static response structural optimization (ESLSO), which is a structural optimization method, is adopted for this formulated optimization [17-19]. An existing method is utilized for RSM.

Equivalent static loads (ESLs) are defined as the loads for linear analysis, which generate the same response field as that of nonlinear analysis. In ESLSO, nonlinear dynamic loads are transformed to ESLs and the ESLs are used as the loading conditions in linear static response optimization. The design is updated in linear static response optimization. Nonlinear analysis is performed with the updated design and the process proceeds in a cyclic manner until the convergence criterion is satisfied. An advantage of ESLSO is that the finite element nodes in the design domain can be controlled easily and exactly in the shape optimization process. However, some design variables cannot be used because only the design variables, which can be defined in linear static response optimization, can be used in optimization using ESLSO [17-23]. New ESLs are proposed to solve the metal forming optimization. Some optimization examples of the sheet metal forming process are defined and solved using the proposed ESLs. Nonlinear dynamic analysis of the sheet metal forming process is performed using the commercial software LS-DYNA [24]. Commercial software NASTRAN [25] is used for the computation of the linear stiffness matrix, which is utilized in the calculation of the ESLs, linear static response analysis and optimization. Commercial software LS-OPT [26] is used for optimization using the RSM. A program is developed to calculate the proposed ESLs, and is interfaced with LS-DYNA and NASTRAN.

2. Metal forming analysis and optimization

2.1 Metal forming analysis

The general tools in the sheet metal forming process are the blank holder, the die and the punch as illustrated in Fig. 1. Generally, the sheet metal is plastically deformed when the

(a) The shape of the blank and the position of the tooling before forming

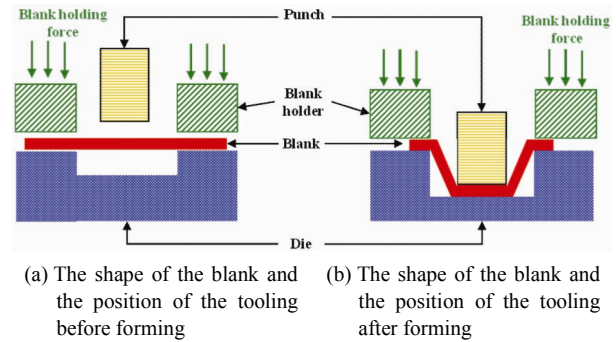(b) The shape of the blank and the position of the tooling after forming

Fig. 1. Schematic view of the tooling when forming the sheet metal.

blank holder and the punch are pressed into the sheet metal. The deformation of a metal depends on the plastic deformation path which is dependent on the strain rate and material properties. The yield strength of a specific area of the sheet metal is reduced by the effects of bending and unbending during the forming process and these effects are called the Bauschinger effect [1, 27, 28]. The used material has a nonlinear stress-strain curve, which is an exponential function for work hardening. Moreover, the material is normal anisotropic material or planar anisotropic material. In forming analysis, the normal anisotropic material is analyzed based on the Hill's theory and that of planar anisotropic material is analyzed by Barlat's yield criterion. In this research, Barlat's yield criterion is adopted. In Barlat's yield criterion, the strain in the 0° direction (the rolling direction), the strain in the 45° direction, the strain in the 90° direction (the transverse direction) and the strain in the thickness direction are not the same [1, 24, 29].

Deformation of the material is generally quite large in the sheet metal forming process, whereas the strains are not relatively large because the change of the surface area and the thickness are not very large. Therefore, the sheet metal forming process is a large deformation and small strain process, and this is a sufficient condition for geometric nonlinearity in analysis. Contact between the metal and the blank holder, the die or the punch occurs, and these contacts are the sources for boundary nonlinearity in analysis. Therefore, computational analysis of the sheet metal forming process depends on time and requires nonlinear dynamic analysis. Finite element analysis is typically employed for the analysis [1, 24, 28].

The sheet metal forming analysis consists of two analyses. They are the forming process analysis and the springback analysis. The springback phenomenon is the elastic restoration of a material after the forming process. When the springback phenomenon occurs, the residual stresses are reduced in each element and the strains and displacements are changed by the reduced stress. For this reason, the dimensions of the product before springback are not the same as those after springback. This phenomenon occurs quite often when the yield strength is large or the stiffness modulus is small. In this research, the forming process and the springback analysis are performed

Table 1. Material properties.

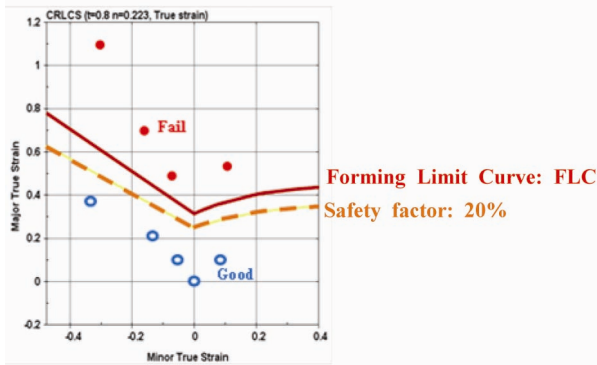|	
Young's modulus (GPa)	E = 207
Poisson's ratio	$\nu = 0.28$
Stress-strain curve (MPa)	$\bar{\sigma} = 648(0.006 + \bar{\varepsilon})^{0.223}$
Lankford value	$R_0 = 1.87$ $R_{45} = 1.27$ $R_{90} = 2.17$
Initial sheet thickness (mm)	0.8

Fig. 2. Forming limit diagram (FLD).

using a commercial finite element software system called LS-DYNA [1, 24].

The failure of a metal can be checked at each element by using the forming limit diagram (FLD) and the FLD is made using the major strain and the minor strain of each element as illustrated in Fig. 2. In FLD, the forming limit curve (FLC) is the failure criterion of the used material. The shape of the FLC is changed by the characteristics of the used metals and the FLC is generally obtained by experiment. The FLC utilized in this research is provided by a commercial software system and is calculated using the thickness and the work hardening coefficient [1, 24]. The used material in Fig. 2 is equal to that of the examples in this research. The material properties of the used sheet metal are summarized in Table 1. The detailed explanation of this material is written in Sec. 4.

2.2 Metal forming optimization

The purpose of the sheet metal forming process is to manufacture the final product which has the desired shape and does not have defects. Optimized structural and process parameters are needed to manufacture the desired final product. The structural parameters such as the initial blank shape can be determined by using various methods. They are the slip line field [2-5], the geometric mapping [9, 10], the plastic deformation theory [11, 12] and the inverse finite element method [6-8]. The process parameters such as BHF, DBRF and DBL can be generally determined by using a probabilistic method (DOE) or an approximation method (RSM) [13, 14].

The slip line field method has some errors because the me-

thod is based on an approximation method. The initial blank shape is determined using the velocities of the nodes. The velocities of the nodes are interpolated from the initial velocity of the punch and the slip line field using an approximation method [2-5]. In the geometric mapping method, the initial blank shape can be obtained through the mapping process, where the desired final shape is projected onto the plane. However, this method has some errors because the plastic deformation of a metal and the geometric constraints cannot be considered exactly [9, 10]. The plastic deformation theory method can determine a more accurate initial blank shape compared to the previous methods and can estimate the strains of the elements in the blank. However, the plastic deformation path of a material is not considered exactly and the Bauschinger effect is ignored in this method [11, 12].

The inverse analysis method is a combination method, which is made by geometric mapping and the plastic deformation theory. If the plastic deformation path of the forming process is complicated, the errors increase when the one-step inverse analysis is used because the plastic deformation path and the blank shape at the mid-step are not estimated exactly. Therefore, the multi-step inverse analysis is typically used to decrease the errors. However, this analysis requires a lot of time and cost compared to the one-step inverse analysis. Also, the multi-step analysis needs the blank shapes at the mid-step because an accurate initial blank shape cannot be determined when the shapes are not expressed exactly [6-8].

In this research, the initial blank shape (structural parameters) is determined using ESLSO. ESLSO is a nonlinear dynamic response optimization method. Nonlinear dynamic analysis and linear static response optimization are involved in ESLSO. It is well known that the process parameters cannot be used as design variables in linear static response optimization. In other words, the design variables must exist in a design object but the process parameters do not exist on the blank. The process parameters should be optimized as well because the desired final forming product is also determined by some process parameters. General researches to optimize the process parameters are conducted by using a probabilistic method or an approximation method. Whereas these methods are not mathematically complicated, they have some errors and require quite a large amount of nonlinear analyses. It is noted that these methods are easier than the conventional optimization method using gradient information and all kinds of design variables can be used. Therefore, the process parameters can be used as design variables in these methods. Moreover, since the number of process parameters is small, these methods can be utilized to determine the process parameters.

Optimization of the sheet metal forming process uses nonlinear dynamic response, so it is nonlinear dynamic response optimization. To overcome the disadvantages of the above mentioned methods, ESLSO is used to optimize the structural parameters in this research. Formulation of the optimization is as follows:

Find $\qquad$ $\mathbf{b} \in \mathrm{R}^n$ $\qquad$ (1a)

to minimize $\qquad$ $f(\mathbf{b})$ $\qquad$ (1b)

subject to $\qquad$ $g_i(\mathbf{b}) \leq 0 \quad (i = 1, 2, \cdots, q)$. $\qquad$ (1c)

Eq. (1) is a formulation to determine the initial blank shape for the final desired shape. $\mathbf{b}$ is the design variable vector for the structural parameters and n is the number of design variables. The design variables are the scale factors for the perturbation vectors, which control the blank shape. The objective function in Eq. (1b) is expressed by the function for the deformed final shape, which can be the mean of radii or the standard deviation of displacements of the selected nodes. The constraints are design specifications including the conditions of the FLD and the desired final shape. The FLD condition is obtained by the characteristics of the used material. The constraints for the desired shape are expressed by the function and they are the standard deviation of radii and the distances between a reference line and the selected nodes. The reference line means the boundary shape of the desired final shape. As mentioned earlier, RSM is used for optimization of the process parameters. The optimization formulation for the process parameters are the same as the one in Eq. (1). Details will be explained later.

3. Optimization methods

As mentioned earlier, the structural parameters are optimized by ESLSO while the process parameters are optimized by RSM. A flow is created to efficiently use the two methods as illustrated in Fig. 3. First, optimization is conducted to determine the structural parameters while the process parameters are set to constants with the current values. Second, the process parameters are optimized with the optimum structural parameters determined in the previous process. The two optimizations are sequentially carried out until the convergence parameters are satisfied as illustrated in Fig. 3. The convergence parameters are defined by the norm of the change of the design variables. It is well known that the optimum solution is a local minimum. At this moment, there is no mathematical optimization method which can find the global minimum point. The only remedy for this is to use many initial design points. The solution in this paper is obtained by many trials of the initial points.

3.1 Non linear static response structural optimization (ESLSO)

ESLSO is made up of two domains which are the analysis domain and the design domain as illustrated in Fig. 4. In the analysis domain, nonlinear analysis such as the metal forming analysis is simulated and the actual nonlinear responses are obtained from this analysis. ESLs are calculated from the nonlinear response vector and the linear stiffness matrix. In the design domain, linear static response optimization is carried out using the calculated ESLs. When linear response analysis is carried out using the ESLs, the nonlinear responses are
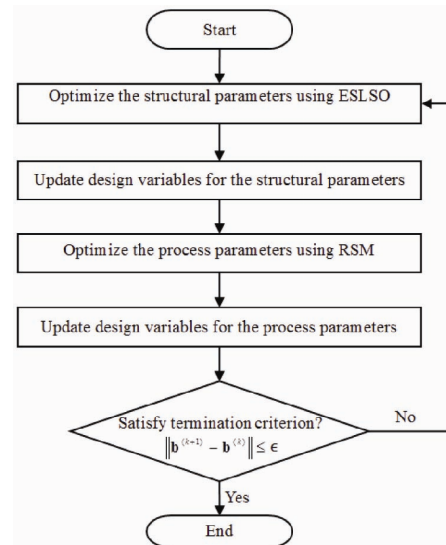

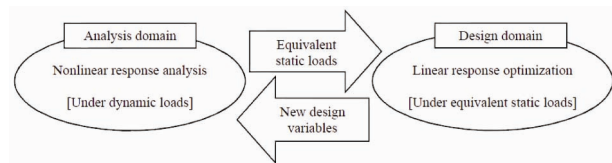Fig. 3. Optimization process using ESLSO and RSM.

Fig. 4. Schematic process between the analysis domain and the design domain.

equal to the linear responses. Therefore, if the ESLs are used as the loading conditions in linear static response optimization, the same responses as the nonlinear responses can be considered at the beginning of linear response optimization. The structural design is updated from linear static response optimization, and nonlinear analysis is performed again using the updated design in the analysis domain. This ESLSO process is repeated until the convergence criterion of the design variables are satisfied [17, 18].

The ESLs for the displacement, which are the static loads, are used to consider the nonlinear dynamic response in linear analysis. When these ESLs are used in linear analysis, the nodal displacement fields from linear analysis are equal to those at the arbitrary time in nonlinear dynamic analysis. In the finite element method, the governing equation of a structure considering nonlinearity in the time domain is

$$\mathbf{M}(\mathbf{b})\ddot{\mathbf{z}}_N(t) + \mathbf{C}(\mathbf{b})\dot{\mathbf{z}}_N(t) + \mathbf{K}(\mathbf{b}, \mathbf{z}_N(t))\mathbf{z}_N(t) = \mathbf{f}(t)$$
$$(t = t_0, t_1, \cdots, t_l) \qquad (2)$$

where $\mathbf{M}$ is the mass matrix and $\mathbf{C}$ is the damping matrix. These matrices are the functions of the design variable vector $\mathbf{b}$. $\mathbf{K}$ is the stiffness matrix which is the function of the design variable vector $\mathbf{b}$ and the nodal displacement vector $\mathbf{z}$. $\ddot{\mathbf{z}}$ is the nodal acceleration vector and $\dot{\mathbf{z}}$ is the nodal

velocity vector. $\mathbf{f}(t)$ is the external load vector and t means the time. The constant l is the total number of the time steps for the numerical integration points. The subscript N means nonlinear dynamic response analysis. $\mathbf{z}_N$ at all the time steps is obtained from Eq. (2).

The equivalent static load vector for the displacement is defined as follows:

$$\mathbf{f}_{eq}^z(s) = \mathbf{K}_L(\mathbf{b})\mathbf{z}_N(s) \qquad (s = 1, 2, \cdots, l) \tag{3}$$

where $\mathbf{f}_{eq}^z(s)$ is the equivalent static load vector for the displacement at each time step. $\mathbf{K}_L$ is the linear stiffness matrix and $\mathbf{z}_N(s)$ is the nodal displacement vector from Eq. (2). The subscript L means linear static analysis. The new notation s is used because the equivalent static load vector is not defined in the time domain and exactly matches with time t. Therefore, the total number of s is l and l equivalent static load vectors are obtained from Eq. (3). $\mathbf{f}_{eq}^z(s)$ is used in linear static analysis as follows:

$$\mathbf{K}_L(\mathbf{b})\mathbf{z}_L(s) = \mathbf{f}_{eq}^z(s) \tag{4}$$

where the linear nodal displacement vector $\mathbf{z}_L(s)$, which is obtained from the linear static analysis using $\mathbf{f}_{eq}^z(s)$, has the same values as the nonlinear nodal displacement vector $\mathbf{z}_N(t)$ in Eq. (3). Therefore, if linear static response optimization is performed using a loading condition of $\mathbf{f}_{eq}^z(s)$, the same nodal displacements as those of the nonlinear dynamic response analysis can be considered in linear static optimization. To consider the time steps of the nonlinear dynamic response analysis, the ESLs sets are calculated for each time step and these sets are used as multiple loading conditions in linear static response optimization. It is well known that many loading conditions can be easily treated in linear static response optimization [24, 25]. Optimization with ESLs for the displacement for metal forming has been proposed by Lee and Park [19].

3.2 Definition of the equivalent static loads for the nonlinear strains

When ESLs for the displacement are used in linear static analysis, the displacement field of nonlinear analysis is the same as that of linear analysis. However, other responses such as stresses and strains do not have the same values in the two analyses. Thus, ESLs for such responses should be newly defined [30]. Since the FLD conditions, which need major and minor strains, are utilized for constraints, ESLs for the strain are made. In other words, ESLs, which can generate the same response field as the strain field of nonlinear analysis, are derived. In ESLSO of the sheet metal forming process, only the final step of the process is considered because the desired shape and the nonlinear strains, which are used the objective function or the constraints in optimization, are the shape and the strains of the final product after the forming process. In

other words, t_f is only considered among the l time steps of Eq. (2) where f means the final time step [19, 27].

In linear static analysis, the linear von-Mises stress and von-Mises strain of an element are expressed as follows [25, 31]:

$$\sigma_L = \frac{1}{\sqrt{2}}\left[(\sigma_x - \sigma_y)^2 + (\sigma_y - \sigma_z)^2 + (\sigma_z - \sigma_x)^2 + 6(\tau_{xy}^2 + \tau_{yz}^2 + \tau_{zx}^2)\right]^{\frac{1}{2}}$$
$$= \sqrt{\frac{(\sigma_x - \sigma_y)^2 + (\sigma_y - \sigma_z)^2 + (\sigma_z - \sigma_x)^2}{2} + 3\tau_{xy}^2} \tag{5}$$

$$\varepsilon_L = \frac{\sqrt{2}}{3}\left[(\varepsilon_x - \varepsilon_y)^2 + (\varepsilon_y - \varepsilon_z)^2 + (\varepsilon_z - \varepsilon_x)^2 + 6(\gamma_{xy}^2 + \gamma_{yz}^2 + \gamma_{zx}^2)\right]^{\frac{1}{2}}$$
$$= \sqrt{\frac{4(\varepsilon_x^2 + \varepsilon_y^2 - \varepsilon_{xy})}{9} + \frac{\gamma_{xy}^2}{3}} . \tag{6}$$

The stress-strain relationship of the isotropic elastic material is expressed from the generalized Hook's law as follows [31]:

$$\begin{Bmatrix} \sigma_x \\ \sigma_y \\ \sigma_z \\ \tau_{xy} \\ \tau_{yz} \\ \tau_{zx} \end{Bmatrix} = \begin{bmatrix} C_{11} & C_{12} & C_{12} & 0 & 0 & 0 \\ C_{12} & C_{11} & C_{12} & 0 & 0 & 0 \\ C_{12} & C_{12} & C_{11} & 0 & 0 & 0 \\ 0 & 0 & 0 & \dfrac{(C_{11}-C_{12})}{2} & 0 & 0 \\ 0 & 0 & 0 & 0 & \dfrac{(C_{11}-C_{12})}{2} & 0 \\ 0 & 0 & 0 & 0 & 0 & \dfrac{(C_{11}-C_{12})}{2} \end{bmatrix} \begin{Bmatrix} \varepsilon_x \\ \varepsilon_y \\ \varepsilon_z \\ \gamma_{xy} \\ \gamma_{yz} \\ \gamma_{zx} \end{Bmatrix} \tag{7a}$$

$$C_{11} = \left[\frac{E}{1+\nu} + \frac{E\nu}{(1+\nu)(1-2\nu)}\right] \tag{7b}$$

$$C_{12} = \frac{E\nu}{(1+\nu)(1-2\nu)} \tag{7c}$$

where E is the Young's modulus and ν is the Poisson's ratio.

The linear von-Mises stress is rewritten using Eq. (7) as follows:

$$\sigma_L = \sqrt{\frac{(C_{11}-C_{12})^2\left[(\varepsilon_x - \varepsilon_y)^2 + (\varepsilon_y - \varepsilon_z)^2 + (\varepsilon_z - \varepsilon_x)^2\right]}{2} + 3\frac{(C_{11}-C_{12})^2}{4}\gamma_{xy}^2}$$
$$= \frac{3}{2}(C_{11}-C_{12})\sqrt{\frac{4(\varepsilon_x^2 + \varepsilon_y^2 - \varepsilon_{xy})}{9} + \frac{\gamma_{xy}^2}{3}} = \frac{3}{2}\frac{E}{1+\nu}\varepsilon_L . \tag{8}$$

From Eq. (8), we have the linear von-Mises stress of the ith finite element as follows:

$$\sigma_{L,i} = \frac{3}{2}\frac{1}{1+\nu}E\varepsilon_{L,i} . \tag{9}$$

The new ESLs are made by modifying the Young's modulus E to E*. With E*, the stiffness matrix is changed from $\mathbf{K}$ to $\mathbf{K}$*. If we conduct linear static analyses with $\mathbf{K}$ and

Table 2. Comparison of the results of two linear analyses with different stiffness matrices.

	Stiffness matrix $\mathbf{K}_L$	Stiffness matrix $\mathbf{K}_L^*$
Calculation the ESLs for the displacements	$\mathbf{f}_{eq} = \mathbf{K}_L \mathbf{z}_N$	$\mathbf{f}_{eq}^B = \mathbf{K}_L^B \mathbf{z}_N$
Linear static analysis using these ESLs	$\mathbf{K}_L \mathbf{z}_L = \mathbf{f}_{eq}$	$\mathbf{K}_L^* \mathbf{z}_L^* = \mathbf{f}_{eq}^*$
Comparison of displacement vectors	$\mathbf{z}_N = \mathbf{z}_L$	$\mathbf{z}_N = \mathbf{z}_L^*$
	$\therefore \mathbf{z}_L = \mathbf{z}_L^*$	
Comparison of linear von-Mises strains	$\varepsilon_{L,i} = \varepsilon_{L,i}^* \quad \left(\because \mathbf{z}_L = \mathbf{z}_L^* \right)$	
Comparison of linear von-Mises stresses	$\sigma_{L,i} \neq \sigma_{L,i}^* \quad \left(\because \mathbf{K}_L \neq \mathbf{K}_L^* \right)$	

$\mathbf{K}^*$, then the two results have the characteristics in Table 2. As shown in Table 2, the two results have different ESLs sets, the same displacement fields, the same von-Mises strain fields and different von-Mises stress fields. Therefore, with E* we have

$$\sigma_{L,i}^* = \frac{3}{2}\frac{1}{1+v}\mathrm{E}_i^*\varepsilon_{L,i}^* = \frac{3}{2}\frac{1}{1+v}\mathrm{E}_i^*\varepsilon_{L,i} \quad \left(\because \varepsilon_{L,i} = \varepsilon_{L,i}^* \right) \qquad (10)$$

where E_i^* is the modified Young's modulus for the ith finite element. It is noted that the von-Mises stress $\sigma_{L,i}^*$ of each element depends on the each Young's modulus E_i^*.

Suppose E_i^* is defined by $\dfrac{\varepsilon_{N,i}}{\sigma_{L,i}}\mathrm{E}$ where $\varepsilon_{N,i}$ is the nonlinear strain of each element from the nonlinear dynamic analysis. $\varepsilon_{N,i}$ can be any major strain or minor strain in nonlinear analysis. Then the modified linear von-Mises stress $\sigma_{L,i}^*$ and the nonlinear strain $\varepsilon_{N,i}$ are the same because

$$\begin{aligned} \sigma_{L,i}^* &= \frac{3}{2}\frac{1}{1+v}\mathrm{E}_i^*\varepsilon_{L,i} = \mathrm{E}_i^*\frac{3}{2}\frac{1}{1+v}\mathrm{E}\varepsilon_{L,i}\frac{1}{\mathrm{E}} \\ &= \mathrm{E}_i^*\frac{\sigma_{L,i}}{\mathrm{E}} = \frac{\varepsilon_{N,i}}{\sigma_{L,i}}\mathrm{E}\frac{\sigma_{L,i}}{\mathrm{E}} = \varepsilon_{N,i} \;. \end{aligned} \qquad (11)$$

In other words, the values of the nonlinear strains are equal to the values of the modified linear von-Mises stresses when E_i^* is used in linear static analysis. Therefore, the constraints with the nonlinear strains can be replaced by the von-Mises stresses in linear static response optimization.

As mentioned earlier, the ESLs for the displacement should be calculated using the displacement at the final step of the nonlinear dynamic analysis. The equivalent static load vector for the displacement $\mathbf{f}_{eq}^f$ can be calculated from Eq. (3) and $\mathbf{f}_{eq}^f$ is used as a loading condition in linear static response optimization. The modified Young's moduli are calculated by the nonlinear strains, the linear von-Mises stresses and the Young's modulus of the workpiece as follows:

$$\mathrm{E}_i^* = \frac{\varepsilon_{N,i}^f}{\sigma_{L,i}}\mathrm{E} \;. \qquad (12)$$

The modified linear stiffness $\mathbf{K}_L^*$ is based on the modified Young's modulus of each element E_i^*.

In the same way, the modified equivalent static load vector for the displacement $\mathbf{f}_{eq}^{f*}$ can be calculated using the modified stiffness matrix $\mathbf{K}_L^*$ and the nonlinear nodal displacement vector $\mathbf{z}_N^f$ at the final step as follows:

$$\mathbf{f}_{eq}^{f*} = \mathbf{K}_L^* \mathbf{z}_N^f \;. \qquad (13)$$

$\mathbf{f}_{eq}^{f*}$ is used as a loading condition in linear static optimization. The modified linear von-Mises stress $\sigma_{L,i}^*$ and the modified linear von-Mises strain $\varepsilon_{L,i}^*$ are calculated from Eq. (13). Two linear von-Mises strain $\varepsilon_{L,i}$ and $\varepsilon_{L,i}^*$ are the same and two linear von-Mises stress $\sigma_{L,i}$ and $\sigma_{L,i}^*$ are different due to the characteristic of the ESLs for the displacements as shown in Table 2. However, the modified linear von-Mises stress $\sigma_{L,i}^*$ is equal to the nonlinear strains $\varepsilon_{N,i}^f$ from Eq. (11). For this reason, $\mathbf{f}_{eq}^{f*}$ is called the equivalent static load vector for the nonlinear strain.

3.3 Optimization using the equivalent static loads for the nonlinear strain

Optimization of the sheet metal forming requires two kinds of nonlinear strain: the major strain and the minor strain. The FLD is defined by the two strains and the failure of the material can be found from the FLD. To consider the two strains in the linear static optimization of ESLSO, two linear finite element models are required because one linear finite element model has one kind of linear von-Mises stress. That is, one finite element model expresses the nonlinear major strain and the other finite element model expresses the nonlinear minor strain as illustrated in Fig. 5. Fig. 6 shows the optimization process of the sheet metal forming process using the ESLs for the nonlinear strains. ε_1 is the major strain and ε_2 is the minor strain, and the steps of this process are as follows:

Step 1 Set values of the initial design variables and parameters (design variables: $\mathbf{b}^{(k)} = \mathbf{b}^{(0)}$, cycle number: $k = 0$, convergence parameter: a small number ε).

Step 2 Perform nonlinear dynamic response analysis. In this step, the linear stiffness matrix and nonlinear responses such as displacements, major strains and minor strains are obtained.

Step 3 Calculate the equivalent static load vector for the displacements at the final step t_l of nonlinear dynamic analysis as follows:

$$\mathbf{f}_{eq}^f = \mathbf{K}_L \mathbf{z}_N^f \;. \qquad (14)$$

Step 4 Solve the linear static analysis as follows:

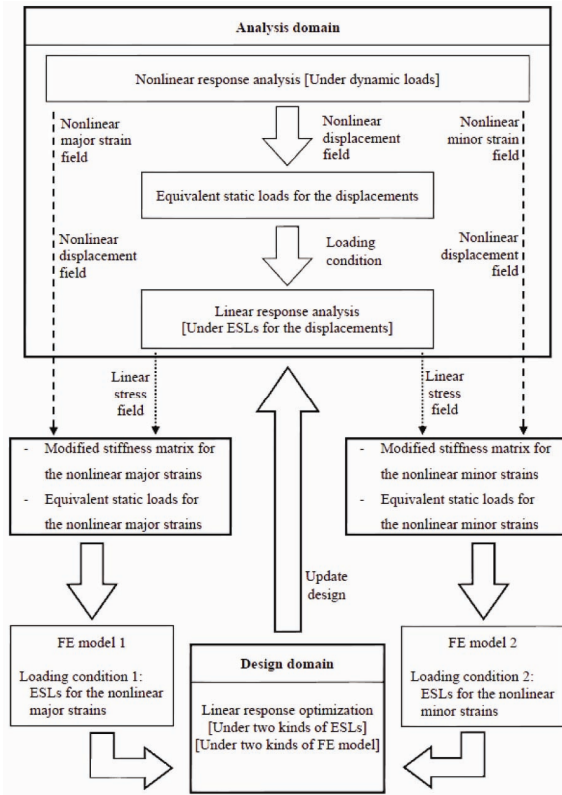$$\mathbf{K}_L \mathbf{z}_L^f = \mathbf{f}_{eq}^f \;. \qquad (15)$$

Fig. 5. Schematic process between the analysis domain and the design domain using two kinds of ESLs for the nonlinear strains.
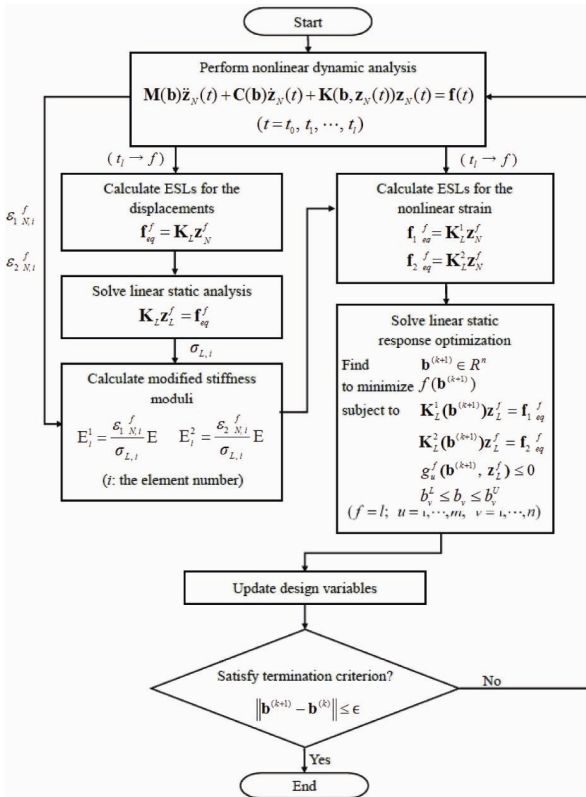

Fig. 6. Optimization process using two kinds of ESLs for the nonlinear strains.

The linear nodal displacement vector $\mathbf{z}_L^f$, the linear von-Mises stresses $\sigma_{L,i}$'s and the linear von-Mises strains $\varepsilon_{L,i}$ are the results of the linear static analysis using $\mathbf{f}_{eq}^f$.

Step 5 Calculate the modified Young's moduli for the two kinds of nonlinear strains as follows:

$$E_i^1 = \frac{\varepsilon_{1\,N,i}^f}{\sigma_{L,i}} E \tag{16a}$$

$$E_i^2 = \frac{\varepsilon_{2\,N,i}^f}{\sigma_{L,i}} E \tag{16b}$$

where i is the element number. E_i^1 is the modified Young's modulus for the nonlinear major strain of each element and E_i^2 is the modified Young's modulus for the nonlinear minor strain of each element. The nonlinear major strain of each element is $\varepsilon_{1\,N,i}^f$ and the nonlinear minor strain of each element is $\varepsilon_{2\,N,i}^f$ from the nonlinear analysis in Step 2. The linear von-Mises stress of each element $\sigma_{L,i}$ is the result of the linear static analysis in Step 4.

Step 6 Calculate the equivalent static load vector for the two kinds of nonlinear strains at the final step t_l of nonlinear dynamic analysis as follows:

$$\mathbf{f}_{1\,eq}^f = \mathbf{K}_L^1 \mathbf{z}_N^f \tag{17a}$$

$$\mathbf{f}_{2\,eq}^f = \mathbf{K}_L^2 \mathbf{z}_N^f \tag{17b}$$

$\mathbf{f}_{1\,eq}^f$ and $\mathbf{K}_L^1$ are the equivalent static load vector and the modified stiffness matrix for the nonlinear major strains, and $\mathbf{f}_{2\,eq}^f$ and $\mathbf{K}_L^2$ are the equivalent static load vector and the modified stiffness matrix for the nonlinear minor strains. $\mathbf{K}_L^1$ and $\mathbf{K}_L^2$ are based on E_i^1 and E_i^2.

Step 7 Solve the following linear static response optimization problem:

$$\text{Find} \quad \mathbf{b}^{(k+1)} \in R^n \tag{18a}$$

$$\text{to minimize} \quad f(\mathbf{b}^{(k+1)}) \tag{18b}$$

$$\text{subject to} \quad \mathbf{K}_L^1(\mathbf{b}^{(k+1)})\mathbf{z}_L^f = \mathbf{f}_{1\,eq}^f \quad (f=l) \tag{18c}$$

$$\mathbf{K}_L^2(\mathbf{b}^{(k+1)})\mathbf{z}_L^f = \mathbf{f}_{2\,eq}^f \quad (f=l) \tag{18d}$$

$$g_u^f(\mathbf{b}^{(k+1)}, \mathbf{z}_L^f) \leq 0 \quad (u=1,2,\cdots,m) \tag{18e}$$

$$b_v^L \leq b_v \leq b_v^U \quad (v=1,2,\cdots,n). \tag{18f}$$

The external load $\mathbf{f}_{1\,eq}^f$ and $\mathbf{f}_{2\,eq}^f$ are the equivalent static load vectors for the nonlinear strains. These vectors are used as the loading conditions during the linear static response optimization process. g means the constraint and m is the number of constraints. The superscript L and U represent the lower and upper bounds, respectively.

Step 8 Update the design results.

Step 9 If

$$\left\| \mathbf{b}^{(k+1)} - \mathbf{b}^{(k)} \right\| \leq \epsilon \tag{19}$$

then terminate the process. Otherwise, set $k = k + 1$ and go to Step 2.

3.4 Optimization process considering both the structural and the process parameters

In the optimization using ESLSO, the structural parameters can only be used because the process parameters cannot be used as the design variables in linear static response optimization. However, process parameters are important variables to obtain the desired final product. In the previous researches, the process parameters are determined using RSM [9, 13, 14].

RSM is an approximation method and used in optimization. The objective function and constraints are approximated to explicit functions and the approximated functions are used in the optimization process. A response surface is interpolated (approximated) by the information of sampled points. The general selection methods of data points are the factorial, composite, D-optimal and Latin Hypercube design [32]. An approximated response surface is generated by using the regression analysis, and the general type of the surface is the linear or the linear with interaction or the quadratic model. The optimum point of RSM is that one point has the best value after comparing the result value of data points and points in the generated surface. This comparing process is necessary because the approximation method has some errors, which are residual between the real data points and the response surface [17, 26]. In this research, an existing RSM in a commercial software system is utilized [26].

When the number of the design variables is small, this method is usefully employed because the number of data points is relatively small. Thus, the process parameters such as BHF, DBRF and DBL can be easily determined using this method. However, using this method is unsuitable in the optimization of the structural parameters because many design variables are required for the desired shape. Therefore, in this research, the structural parameters are optimized using ESLSO and the process parameters are optimized using RSM. The optimization method using both ESLSO and RSM in Fig. 3 is a new optimization concept which is to consider the characteristics of the design variables.

4. Optimization of the proposed method with examples

Two example problems for the sheet metal forming process are solved by using the proposed method. One is shape optimization of the blank and the other is optimization for both the blank shape and process conditions. The first example has only structural parameters and the second one has structural and process parameters. The objective functions are the desired shapes after the forming process, and they are expressed by the functions of the displacements. The material properties of the used sheet metal are summarized in Table 1. The utilized metal is a planer anisotropic material under plane stress conditions and the used yield criterion is Barlat's yield crite-
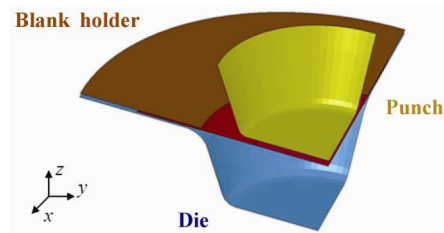

Fig. 7. Tooling of the circular cup.

rion [1, 24]. As mentioned earlier, LS-DYNA is employed for nonlinear dynamic analysis [24] and NASTRAN is employed for linear static response optimization at each cycle in ESLSO. The optimization algorithm in NASTRAN is based on the feasible directions method [25, 33].

4.1 Optimization of the circular cup

This example is shape optimization of the sheet metal forming of the circular cup. The parameters, which are used as the design variables in ESLSO, are the curvature and radii of the initial blank. The parameters are the structural parameters because the blank shape is expressed by the values of the curvature and radii. The tooling for the sheet metal forming of the circular cup consists of the die, the punch and the blank holder as illustrated in Fig. 7. The punch velocity and the blank holding force are constant. The die is fixed and the stroke of the punch is 40 mm. The static friction factor is set to 0.125 and the dynamic friction factor is set to 0.12. A quarter of the circular cup is used for the shape of the used model in nonlinear dynamic analysis and linear static response optimization.

Nonlinear dynamic analysis includes the manufacturing process and the springback [24]. The used nonlinear responses are at the final step of nonlinear analysis after the springback phenomenon for the elastic recovery of the material [1]. In this example, the ESLs for the nonlinear strain are made in ESLSO and these ESLs are generated by the major strains, minor strains and displacements from the nonlinear dynamic analysis.

Fig. 8 is the results of the nonlinear dynamic analysis when the radius of the initial blank is 64 mm. Fig. 8(a) is the maximum major strain contour for the forming limit curve (FLC) and Fig. 8(b) is the forming limit diagram (FLD). The failure criterion is 1.0 and failure of the material occurs at the bottom of the wall as illustrated in Fig. 8(a). The failure parts are shown in Fig. 8(b) [1, 7, 24].
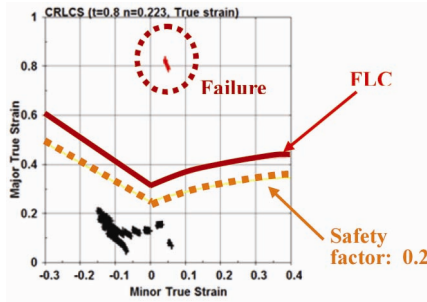
The objective function is maximization of the radius at the edge of the flange. The constraints are the FLD conditions of all the finite elements and the shape of the flange edge. The radius of the used initial blank is 50mm. The formulation of the optimization is as follows:

Find b_1, b_2, b_3 (20a)
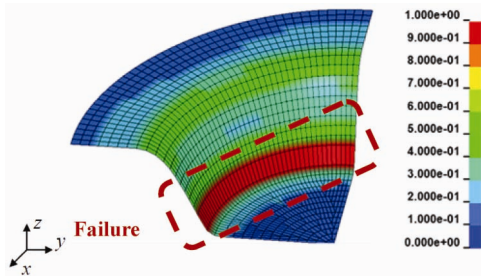
(a) The maximum major strain contour for the forming limit curve

(b) Forming limit diagram

Fig. 8. Results of nonlinear dynamic response analysis of the circular cup (initial blank radius: 64 mm).
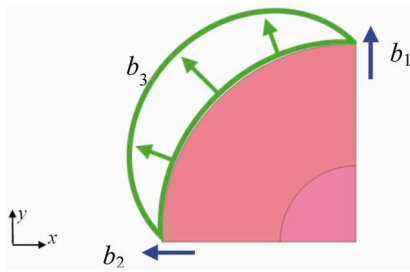

Fig. 9. The initial blank shape and design variables of the circular cup.

$$\text{to minimize} \quad -m_1 \tag{20b}$$

$$\text{subject to} \quad \varepsilon_1 < -0.626\varepsilon_2^2 + 0.552\varepsilon_2 + 0.312 \tag{20c}$$
$$(\text{if } \varepsilon_2 \geq 0.1)$$

$$\varepsilon_1 < -\varepsilon_2 + 0.312 \qquad (\text{if } \varepsilon_2 \leq -0.1) \tag{20d}$$

$$\varepsilon_1 < 0.312 - 0.236\varepsilon_2 + 14.237\varepsilon_2^2$$
$$- 2.348\varepsilon_2^3 - 970.0\varepsilon_2^4$$
$$+ 39.125\varepsilon_2^5 + 29100.0\varepsilon_2^6 \tag{20e}$$
$$(\text{if } -0.1 < \varepsilon_2 < 0.1)$$

$$0.0 \leq s_1 \leq 0.5 \tag{20f}$$

where, b_1, b_2 and b_3 are the scale factors of the perturbation vectors (shape variables) as illustrated in Fig. 9. The radii and curvature of the design domain in the blank are controlled by the perturbation vectors. The vectors are determined based on the Lankford value because the used material is a planner anisotropic material and has a different strain at each direc-

tion; the base directions of the Lankford value are $0°$, $45°$ and $90°$ for the rolling direction. The used Lankford value is expressed in Table 1. m_1 is the expected value of the radii of the sampled nodes in the flange edge after deformation. The constraint m_1 is defined as follows:

$$m_1 = \frac{1}{46}\sum_{r=1}^{46} R_r \tag{21}$$

where 46 for r is the number of sampled nodes of the flange edge and R_r is the radius of the r th sampled node.

The reason why the expected value of the radii is maximized is that a large flange can have a failure at the wall of the cup while a large flange is sometimes required to attach accessories on it. Although a large flange is desirable, it is difficult for a designer to identify how large it can be. We can define the objective function with a desirable target for the magnitude of the flange, however, this work has already been done in other research [19, 34].
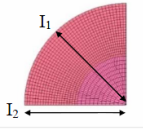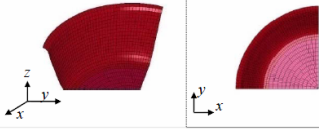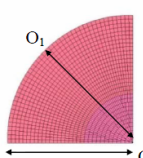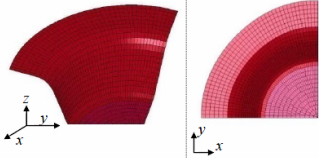
ε_1 is the major strain and ε_2 is the minor strain from nonlinear dynamic analysis. The original FLC cannot be directly used in linear static response optimization because the point where the minor strain is zero is a non-differentiable point as illustrated in Fig. 8(b). So the FLC is interpolated to be differentiable at all the points. The interpolated curve is expressed by three conditions in the constraints, which are Eqs. (20c)-(20e). These constraints for the nonlinear strains are used for the von-Mises stresses of linear static analysis in the design domain when the ESL for the nonlinear strains is used in ESLSO. s_1 is the standard deviation of the radii of the sampled nodes and defined as:
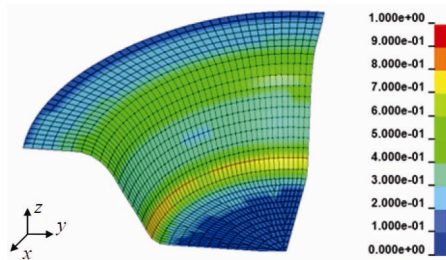
$$s_1 = \sqrt{\frac{1}{45}\sum_{r=1}^{46}(R_r - m_1)^2} \, . \tag{22}$$

The convergence criterion is 0.001. The optimization process converges at the 29th cycle. The infinite norm of the design variables is 0.0. Table 3 shows the shape comparison of the initial model and the optimum model. The radii of the sampled nodes in the optimum model are not the same because the strain in each direction is not the same due to Barlat's yield criterion. Fig. 10 shows the nonlinear analysis results of the optimum model. Fig. 10(a) is the maximum major strain contour for the FLC and Fig. 10(b) is the FLD. The objective function decreases from -40.033 to -57.088 and the history of the objective function is illustrated in Fig. 11. The constraint violation decreases from 19.3% to 0.0%. The initial blank shape, which can be deformed to the desired shape without failure, is determined.
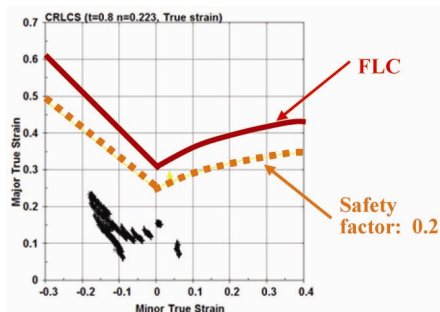
The friction factor is an important parameter determining the optimum blank shape in the sheet metal forming process. The optimum models are changed according to the friction factors. Table 4 shows the comparison of the optimum shapes of each friction factor. When friction is large, the area of the

Table 3. Shape comparison of the circular cup between the initial model and the optimum model.

	Initial blank shape	Shape of blank after the sheet metal forming	
Initial model	I₁ (image) I₂	(formed shape image)	(detail image)
	I$_1$: 50 mm I$_2$: 50 mm	Expected value of the outer radii : 40.033 mm	
Optimum model	O₁ (image) O₂	(formed shape image)	(detail image)
	O$_1$: 62.59 mm O$_2$: 61.55 mm	Expected value of the outer radii : 57.088 mm	

Table 4. The comparison of the optimum shapes of each friction factor.

Friction factor	Initial blank shape [Optimum model]	Shape of blank after the sheet metal forming	
Friction type A μ_{static} : 0.125 $\mu_{dynamic}$: 0.12	A1 (image) A2	(formed shape image)	(detail image)
	A1: 62.59mm A2: 61.55mm	Expected value of the outer radii : 57.088mm	
Friction type B μ_{static} : 0.14 $\mu_{dynamic}$: 0.135	B1 (image) B2	(formed shape image)	(detail image)
	B1: 60.65mm B2: 58.13mm	Expected value of the outer radii : 54.392mm	
Friction type C μ_{static} : 0.155 $\mu_{dynamic}$: 0.15	C1 (image) C2	(formed shape image)	(detail image)
	C1: 56.31mm C2: 54.23mm	Expected value of the outer radii : 48.837mm	

(a) The maximum major strain contour for the forming limit curve

(b) Forming limit diagram

Fig. 10. Results of nonlinear dynamic response analysis using the optimum model of the circular cup.
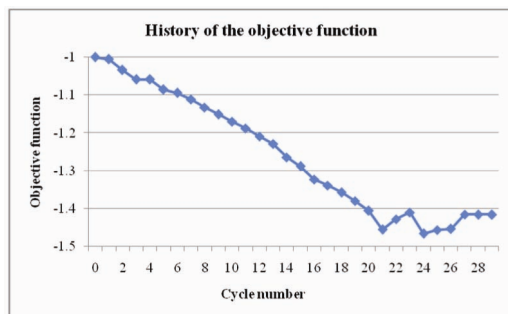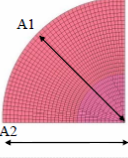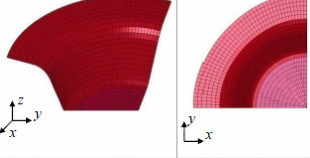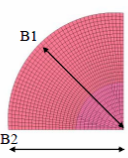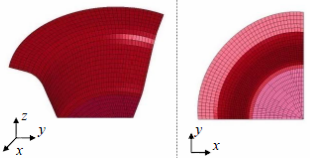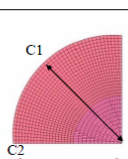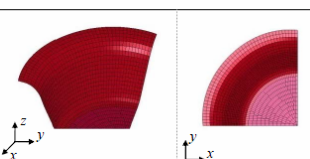

Fig. 11. History of the objective function of the circular cup.

initial blank and the radius of the flange edge of the deformed shape become smaller because the strains are large and the necking occurrence probability is high. The friction factor is not used as the design variable in this research. Further in-depth research on the friction factor is required.

4.2 Optimization of the square cup

This example, which is an optimization of the square cup, consists of an optimization for the structural parameters using ESLSO and an optimization for the process parameters using RSM. The structural parameters are curvatures, angles and radii of the initial blank and the process parameters are BHF, DBRF and DBL [1, 14-16, 26]. The two optimization processes iteratively proceeds until the convergence criteria are satisfied as illustrated in Fig. 3.

Sequential response surface method (SRSM), which is one of the RSMs, is used in this example. SRSM uses the region of interest, which is a subspace of the design space, to determine an approximate optimum value. The initial size of the region is made by the lower and upper bounds of the design variables. After the optimization process, the center of the region is moved and the size of the region is reduced. This process is repeated until the convergence criteria are satisfied. The used selection method of data points is the D-optimal method and the order of the used model is quadratic in this example [26].

The tooling for the sheet metal forming of the square cup consists of the die, the punch and the blank holder as illustrated in Fig. 12(a). The punch velocity is constant. The die is fixed and the stroke of the punch is 40 mm. The static friction factor is 0.125 and the dynamic friction factor is 0.12. The used model, which is used in nonlinear dynamic analysis and linear static response optimization, is a quarter of a square cup. Nonlinear dynamic analysis includes the manufacturing process and the springback. The ESLs for the nonlinear strain are employed in linear static optimization of ESLSO [1, 7, 24].

The objective function is wrinkling reduction at the edge of the flange. The constraints are the FLD conditions and the shape of the flange edge. The radius of the initial blank is 90mm. The optimization formulation for the structural parameters is as follows:

(a) The tooling and the process parameters

(b) The initial blank shape and the structural parameter

Fig. 12. Model of the sheet metal forming of the straight square cup.

$$\text{Find} \quad b_i \quad (i=1, 2, 3, \cdots, 15) \quad (23a)$$

$$\text{to minimize} \quad s_2 \quad (23b)$$

$$\text{subject to} \quad -0.3 \le D_w \le 0.3 \quad (w=1, 2, 3, \cdots, 51) \quad (23c)$$

$$\varepsilon_1 < -0.626\varepsilon_2^2 + 0.552\varepsilon_2 + 0.312$$
$$(if \ \varepsilon_2 \ge 0.1) \quad (23d)$$

$$\varepsilon_1 < -\varepsilon_2 + 0.312 \quad (if \ \varepsilon_2 \le -0.1) \quad (23e)$$

$$\varepsilon_1 < 0.312 - 0.236\varepsilon_2 + 14.237\varepsilon_2^2$$
$$- 2.348\varepsilon_2^3 - 970.0\varepsilon_2^4$$
$$+ 39.125\varepsilon_2^5 + 29100.0\varepsilon_2^6 \quad (23f)$$
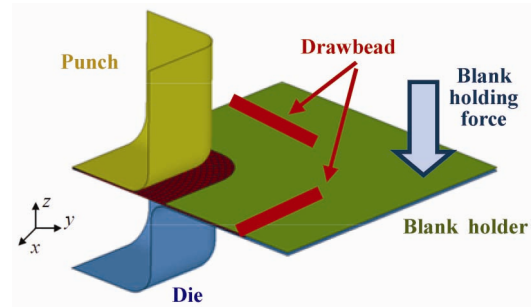$$(if \ -0.1 < \varepsilon_2 < 0.1)$$

where $b_1, b_2, \cdots, b_{15}$ are the scale factors of the perturbation vectors as illustrated in Fig. 12(b) and these design variables are used in linear static optimization of ESLSO. The radii and curvature of the design domain in the blank are controlled by the perturbation vectors. s_2 is the standard deviation and is used to reduce wrinkling. It is calculated from the displacement in the z-direction of the sampled nodes at the flange part. The standard deviation is minimized to make the edge flat. s_2 is defined as follows:

Fig. 13. Deformed shape of a wrinkled square cup.

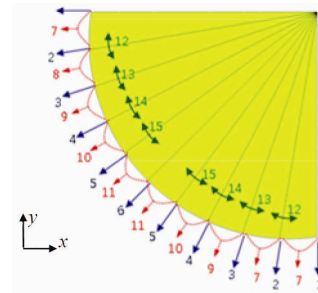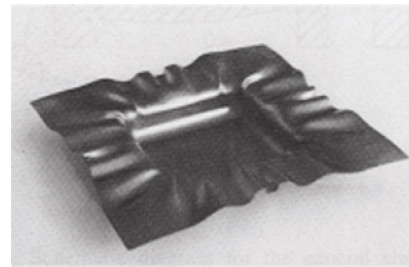$$s_2 = \sqrt{\frac{1}{152}\left(\sum_{k=1}^{153}(z_k - \bar{z})^2\right)} \quad (24)$$

where z_k is the displacement in the z-direction of the kth sampled node and $\bar{z}$ is the expected value of z's.

The constraint D_w is the distance between the target line and the deformed position at the wth edge node as illustrated in Fig. 14. The target line is the desired final shape of the flange edge, which is desired radius at the sampled node. The target means the nodal coordinate of the desired shape. The constraint D_w is defined as follows:

Fig. 14. The constraint of the straight square cup.

$$D_w = \left| R_T - \sqrt{x_w^2 + y_w^2} \right| \quad (w=1, 2, 3, \cdots, 51) \quad (25)$$

where R_T is the target radius of the flange edge after the forming process. x_w is the coordinate of the deformed position in the x-direction and y_w is the coordinate of the deformed position in the y-direction at the wth edge node after the forming process. This constraint is used to obtain the desired planar shape of the final product. Eqs. (23d)-(23f) are the interpolated FLD condition.

Wrinkling generally occurs when BHF is weak, and Fig. 13

Fig. 15. Schematic view of the drawbead.

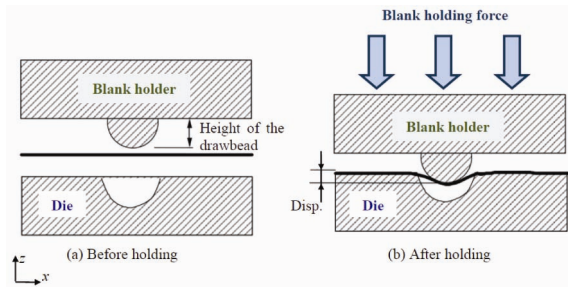shows the deformed shape of a wrinkled square cup. Then, the wrinkling can be controlled by BHF. If BHF is too large, the wrinkling is reduced but necking may occur in the wall of the forming product. Therefore, when BHF is fixed, wrinkling can be controlled by the blank shape in the first stage of Fig. 3 although the impact is not very large. In the second stage, RSM is used to determine BHF and DBRF and the objective is to minimize the wrinkle. As illustrated in Fig. 3, the two stages are repeatedly used until the convergence criterion is satisfied. It is noted that BHF and DBRF are coupled. They are independently considered in this research. Since those variables are simultaneously considered as design variables in the second stage (RSM), the decision of a variable is dependent on the decision of the other variable. Therefore, they are not independently determined.

The formulation of the RSM to optimize the process parameters is as follows:

$$\text{Find} \quad b_h \qquad (h = 16, 17, 18) \qquad (26a)$$
$$\text{to minimize} \quad s_2 \qquad (26b)$$
$$\text{subject to} \quad -0.3 \le D_w \le 0.3 \quad (w = 1, 2, 3, \cdots, 51) \qquad (26c)$$
$$\varepsilon_1 < -0.626\varepsilon_2^2 + 0.552\varepsilon_2 + 0.312 \qquad (26d)$$
$$(if \ \varepsilon_2 \ge 0.0)$$
$$\varepsilon_1 < -\varepsilon_2 + 0.312 \quad (if \ \varepsilon_2 < 0.0) \qquad (26e)$$

where b_{16}, b_{17} and b_{18} are the design variables of the process parameter and they are BHF, DBRF and DBL, respectively. As mentioned earlier, the commercial software LS-OPT is utilized to solve the problem of Eq. (26) [26]. The FLD constraint in LS-OPT uses real FLC of material. Therefore, the interpolated curves, which are used in ESLSO, are not used in RSM. The objective function and the constraint for the plane shape are equal to those of ESLSO.

The convergence criterion of ESLSO is defined as 0.01 and the convergence criterion of RSM is defined as 0.03. The total optimization process converges in the 3rd cycle. The history of the optimization results is shown in Table 5. The objective function decreases from -40.033 to -57.088 and the constraint violation decreases from 18343.0% to 0.0%. Figs. 16 and 17 show the results of the initial model and the optimum model. Fig. 16 presents the initial and deformed blank shapes of the

Table 5. History of the optimization results of the square cup.

| Design cycle | Data point | Process parameter | | | Structural parameter | Objective function | The number of nonlinear analyses |
		DBL (mm)	DBRF (N/mm)	BHF (kN)	Infinite norm of the design variables		
Initial		30.00	100.00	15.00		1.000	
#1 ESLSO		30.00	100.00	15.00	0.0013	1.052	9
#1 RSM	Iter. 1 – point 7	10.00	50.00	15.00		0.535	17
	Opt. point	16.12	50.00	14.63		0.616	
#2 ESLSO		10.00	50.00	15.00	0.0066	0.500	20
#2 RSM	Iter. 6 – point 3	11.70	50.00	16.47		0.419	97
	Opt. point	12.83	50.00	16.87		0.430	
#3 ESLSO		11.70	50.00	16.47	0.0049	0.465	21
#3 RSM	Iter 1 – point 1	11.70	50.00	16.47		0.465	33
	Opt. point	10.00	54.09	15.08		0.576	
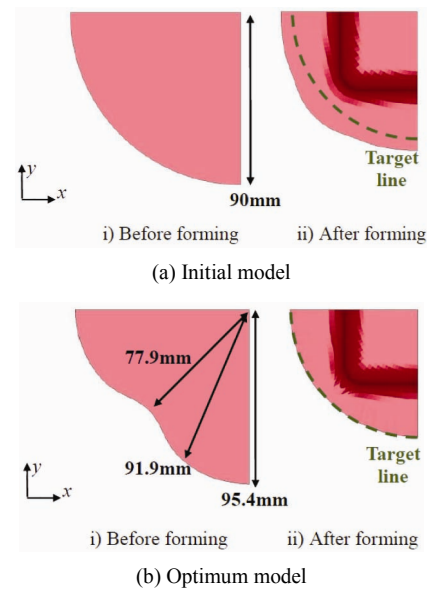
Fig. 16. The initial blank shape and the deformed blank shape of the square cup.

initial and the optimum models. Fig. 17 illustrates the maximum major strain contour for the FLC and the FLD of each model.

5. Conclusions

The optimization process of sheet metal forming, which has

(a) The maximum major strain contour for the forming limit curve of the initial model

(b) The maximum major strain contour for the forming limit curve of the optimum model

(c) Forming limit diagram of the initial model

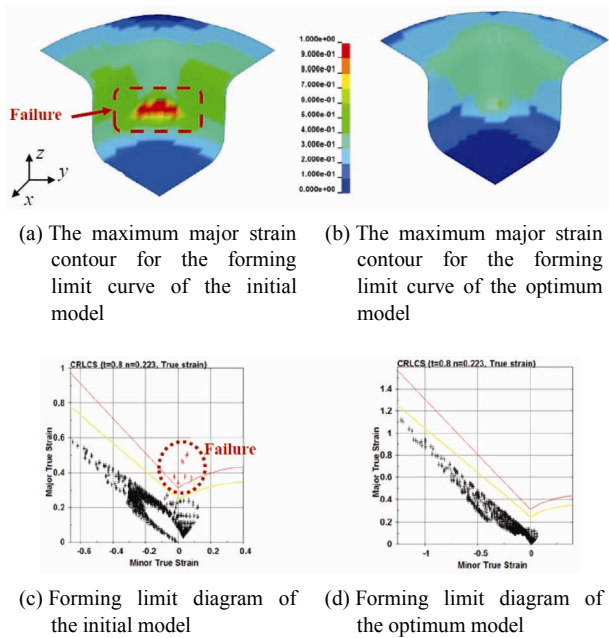(d) Forming limit diagram of the optimum model

Fig. 17. The result contours and FLD of the initial model and the optimum model.

geometric, material and boundary nonlinearities in finite element analysis, is nonlinear dynamic response optimization. The final shape after the forming process is affected by the structural and the process parameters. These parameters have been generally optimized using an interpolation method, a probabilistic method, an approximation method, etc. However, it is quite difficult to optimize both the structural and the process parameters simultaneously because the number of design variables is large and errors may increase. A design method is proposed to optimize both parameters by using ESLSO and RSM.

ESLSO can be applied to nonlinear dynamic response optimization using the linear static response optimization technique. The design variables, which can be used in linear static response optimization, can only be considered in ESLSO. Typically, structural parameters are such variables. On the other hand, the process variables, which cannot be used in linear static response optimization, are optimized using RSM. That is, ESLSO is used to optimize the structural parameters and RSM is used to optimize the process parameters. The two optimization processes proceeds iteratively until the convergence criteria are satisfied.

Material failure, which influences the quality of the final product, is considered in the optimization of the sheet metal forming process. However, ESLSO using the ESLs for the displacement cannot be directly utilized because material failure is the function of the nonlinear strain. Therefore, the ESLs for the nonlinear strain are proposed and the nonlinear strains from nonlinear dynamic analysis are considered using these ESLs in linear static response optimization of ESLSO. Two examples are successfully solved by using the proposed me-

thod. However, various nonlinear conditions are not yet considered. Also, the objective and constraint functions which have practical meanings should be considered later. Extension of the current research is required to solve such problems.

Acknowledgment

Nomenclature———————————————

$\mathbf{b}$	: Design variable vector
$\mathbf{C}$	: Damping matrix
D_w	: Distance between the target line and the deformed position at the wth edge node
E	: Young's modulus
E^*	: Modified Young's modulus
E_i^*	: Modified Young's modulus for the ith finite element
$\mathbf{f}$	: External load vector
f	: Final step (superscript)
$\mathbf{f}_{eq}^{\mathbf{z}}$	: Equivalent static load vector for the displacement
$\mathbf{f}_{eq}^{f*}$	: Equivalent static load vector for the nonlinear strain at the final step
g	: Constraint
$\mathbf{K}$	: Stiffness matrix
$\mathbf{K}_L$	: Linear stiffness matrix
$\mathbf{K}^*$	: Modified stiffness matrix
k	: Cycle number
L	: Linear static analysis
L	: Lower bound (Superscript)
l	: Total number of the time steps for the numerical integration points
$\mathbf{M}$	: Mass matrix
m	: Number of constraints
m_1	: Expected value of the radii of the sampled nodes
N	: Nonlinear dynamic response analysis
n	: Number of design variables
R	: Lankford value
R_r	: Radius of the r th sampled node
R_T	: Target radius of the flange edge after the forming process
s_1	: Standard deviation of the radii of the sampled nodes
s_2	: Standard deviation of the z-direction displacement of the sampled nodes
t	: Time
U	: Upper bound (Superscript)
x_w	: Coordinate of the deformed position in the x-direction at the wth edge node after the forming process
y_w	: Coordinate of the deformed position in the y-

direction at the *w*th edge node after the forming process

$\mathbf{z}$: Nodal displacement vector

$\dot{\mathbf{z}}$: Nodal velocity vector

$\ddot{\mathbf{z}}$: Nodal acceleration vector

$\bar{z}$: Expected value of the sampled nodes

z_k : Displacement in the z-direction of the *k*th sampled node

$\bar{\varepsilon}$: Effective strain

ε_L : Linear von-Mises strain

ε_1 : Major strain

ε_2 : Minor strain

ϵ : Convergence parameter

ν : Poisson's ratio

$\bar{\sigma}$: Effective stress

σ_L : Linear von-Mises stress

References

[1] W. F. Hosford and R. M. Caddell, *Metal forming: Mechanics and metallurgy*, Cambridge University Press, New York, USA (2011).

[2] M. Karima, Blank development and tooling design for drawn parts using a modified slip line field based approach, *Journal of Engineering for Industry*, 111 (1989) 345-350.

[3] M. S. Kim, J. H. Shin and D. G. Seo, Formability of sheet metal in noncircular cup (II) – for arbitrary cross section, *Transactions of the Korea Society of Mechanical Engineers*, 17 (12) (1993) 3074-3104 (in Korean).

[4] J. H. Shin, M. S. Kim and D. K. Seo, Formability of sheet metal in noncircular cup drawing (I) – for rectangular cross section, *Transactions of the Korean Society of Automotive Engineers*, 2 (1) (1994) 84-95 (in Korean).

[5] X. Chen and R. Sowerby, Blank development and the prediction of earing in cup drawing, *Journal of Mechanical Sciences*, 38 (5) (1996) 509-516.

[6] C. H. Lee and H. Huh, Blank design and strain prediction of automobile stamping parts by an inverse finite element approach, *Journal of Materials Processing Technology*, 63 (1997) 645-650.

[7] C. H. Lee and H. Huh, Three-dimensional multi-step inverse analysis for the optimum blank design in sheet metal forming processes, *Journal of Materials Processing Technology*, 80-81 (1998) 76-82.

[8] C. Lee and J. Cao, Shell element formulation of multi-step inverse analysis for axisymmetric deep drawing process, *International Journal for Numerical Method in Engineering*, 50 (2001) 681-706.

[9] J. H. Vogel and D. Lee, An analysis method for deep drawing process design, *International Journal of Mechanical Sciences*, 32 (1990) 891-907.

[10] X. Chen and R. Sowerby, The development of ideal blank shapes by the method of plane stress characteristics, *Journal of Mechanical Sciences*, 34 (2) (1992) 159-166.

[11] R. Sowerby, J. L. Duncan and E. Chu, The modeling of sheet metal stamping, *Journal of Mechanical Sciences*, 28 (7) (1986) 415-430.

[12] G. N. Blount and P. R. Stevens, Blank shape analysis for heavy gauge metal forming, *Journal of Materials Processing Technology*, 24 (1990) 65-74.

[13] S. Chengzhi, C. Guanlong and L. Zhongqin, Determining the optimum variable blank-holder forces using adaptive response surface methodology (ARSM), *International Journal of Advanced Manufacturing Technology*, 26 (2005) 23-29.

[14] W. Zhang and R. Shivpuri, Probabilistic design of aluminum sheet drawing for reduced risk of wrinkling and fracture, *Reliability Engineering and System Safety*, 94 (2009) 152-161.

[15] X. Wang and J. Cao, Stress-based prediction for the straight side-wall wrinkling in deep drawing process, *Transactions of NAMRI/SME*, 27 (1999) 55-60.

[16] R. Shivpuri and W. Zhang, Robust design of spatially distributed friction for reduced wrinkling and thinning failure in sheet drawing, *Material and Design*, 30 (6) (2009) 2043-2055.

[17] G. J. Park, *Analytical methods for design practice*, Springer-Verlag, Berlin, Germany (2007).

[18] W. S. Choi and G. J. Park, Structural optimization using equivalent static loads at all the time intervals, *Computer Methods in Applied Mechanics and Engineering*, 191 (19) (2002) 2077-2094.

[19] J. J. Lee and G. J. Park, Shape optimization of the initial blank in the sheet metal forming process using equivalent static loads, *International Journal for Numerical Methods in Engineering*, 85 (2) (2011) 247-268.

[20] G. J. Park and B. S. Kang, Validation of a structural optimization algorithm transforming dynamic loads into equivalent static loads, *Journal of Optimization Theory Application*, 118 (1) (2003) 191-200.

[21] B. S. Kang, G. J. Park and J. S. Arora, Optimization of flexible multibody dynamic systems using the equivalent static load, *AIAA Journal*, 43 (4) (2005) 846-852.

[22] M. K. Shin, K. J. Park and G. J. Park, Optimization of structures with nonlinear behavior using equivalent loads, *Computer Methods in Applied Mechanics and Engineering*, 196 (4) (2007) 1154-1167.

[23] Y. I. Kim and G. J. Park, Nonlinear dynamic response structural optimization using equivalent static loads, *Computer Methods in Applied Mechanics and Engineering*, 199 (2010) 660-676.

[24] LS-DYNA, *LS-DYNA User's Manual Version 971*, Livermore Software Technology Corporation, Livermore, California, USA (2013).

[25] NASTRAN, *MD R3 NASTRAN User's Guide*, MSC Software Corporation, Santa Ana, California, USA (2012).

[26] LS-OPT, *LS-OPT User's Manual Version 4.2*, Livermore Software Technology Corporation, Livermore, California, USA (2012).

[27] J. H. Lim, S. B. Kim, J. S. Kim, H. Huh, J. D. Lim and S. H. Park, High speed tensile tests of steel sheets for an auto-body at the intermediate strain rate, *Transactions of the Korea So-*

ciety of Automotive Engineers, 13 (2) (2005) 127-134 (in Korean).

[28] R. W. Cahn and P. Haasen, *Physical Metallurgy*, North-Holland, Amsterdam, Netherlands (1996).

[29] J. N. Reddy, *An introduction to nonlinear finite element analysis*, Oxford University Press, New York, USA (2005).

[30] J. J. Lee, U. J. Jung and G. J. Park, A preliminary study on the optimal preform design in the forging process using equivalent static loads, *13th AIAA/ISSMO Multidisciplinary Analysis and Optimization Conference*, Fort Worth, Texas, USA (2010).

[31] A. C. Ugural and S. K. Fenster, *Advanced strength and applied elasticity*, Prentice Hall, Upper Saddle River, New Jersey, USA (2003).

[32] R. H. Myers and D. C. Mongomery, *Response surface methodology*, John Wiley and Sons. Inc., Hoboken, New Jersey, USA (2009).

[33] A. D. Belegundu and T. R. Chandrupatla, *Optimization Concepts and Applications in Engineering*, Cambridge University Press, New York, USA (2011).

[34] J. J. Lee, U. J. Jung and G. J. Park, Shape optimization of the workpiece in the forging process using equivalent static loads, *Finite Element in Analysis and Design*, 69 (2013) 1-18.

Jae-Jun Lee received the B.S. degree in mechanical engineering from Yeungnam University, Korea, in 2004, M.S. degree from Hanyang University, Korea, in 2006, and the Ph.D. from Hanyang University, Korea, in 2011. In 2006-2007, he worked as an engineer at Hyundai DYMOS, Korea. He is currently a senior researcher in the Nuclear Fuel Engineering Dept. at KEPCO Nuclear Fuel, Daejeon, Korea.

Gyung-Jin Park received the B.S. degree from Hanyang University, Korea in 1980, M.S. degree from KAIST, Korea, in 1982, and the Ph.D. from the University of Iowa, USA, in 1986. In 1986-1988, he worked as an assistant professor at Purdue University at Indianapolis, USA. His research focuses on Structural Optimization, machine design, design theory and MDO. His work has yielded over 4 books and 360 technical papers. He is currently a professor in the Department of Mechanical Engineering at Hanyang University, Ansan City, Korea.